Theoretical Study of the Dipole-Bound Excited States of $I^-(H_2O)_4$

Fernando D. Vila† and Kenneth D. Jordan*

Department of Chemistry and Center for Molecular and Materials Simulations, University of Pittsburgh, Pittsburgh, Pennsylvania 15260

Received: August 17, 2001; In Final Form: December 3, 2001

Photoexcitation of $I^-(H_2O)_n$ clusters can lead to charge transfer states with the excess electron localized on the water cluster, making these ideal systems for studying electron/water cluster dynamics. In the present study, the MP2 method is used to study the structure and infrared spectrum of the ground state of $I^-(H_2O)_4$ and the CASPT2 method is used to characterize the low-lying electronically excited states of the complex. The calculated IR spectrum is in good agreement with experimental results, providing support for a crown-like structure of $I^-(H_2O)_4$. The 2^1A excited state is predicted to be 29 meV below the ground state of the neutral cluster (at the geometry of the ground-state anion), and the vertical excitation energy for the $1^1A \rightarrow 2^1A$ charge-transfer transition is calculated to be 4.60 eV, in good agreement with the experimental value of 4.5 eV. Potential energy curves for the relaxation of the photoexcited $I^-(H_2O)_4$ cluster from the crown-like to the planar structure are presented.

Introduction

The nature of excess electrons in liquid water has long been the subject of intense experimental[1−8] and theoretical[9−12] investigation. Photoexcitation of I^-(aq) has proven to be a particularly valuable approach to the study of the dynamics of excess electrons in water, as the photoexcitation process produces charge transfer states with the excess electron delocalized in the water.[13−15] In recent years, much attention has been focused on negatively charged water clusters.[16−32] Here too, the introduction of an I^- ion has proven useful for probing the dynamics of the excess electron.[33−35] Serxner et al.[33] have found that upon photoexcitation the $I^-(H_2O)_{n=2-6}$ clusters undergo charge transfer from the I^- to the water cluster. Subsequently, Lehr et al.[34] used femtosecond photoelectron spectroscopy to probe the solvation dynamics of photoexcited $I^-(H_2O)_{n=4-6}$ clusters, and found that, although the $n = 4$ cluster has a simple population decay, the $n = 5$ and 6 clusters exhibit more complicated dynamics. This was taken as evidence of a rearrangement of the water molecules that stabilizes the excited electron in the larger clusters.[34]

The experimental work of Lehr et al. was followed by theoretical studies of $I^-(H_2O)_4$ by Kim et al.[36] and $I^-(H_2O)_{n=4-6}$ by Chen and Sheu.[37,38] Both of these studies reported vertical excitation energies for the charge-transfer states. Chen and Sheu also considered the role of geometrical relaxation following photoexcitation.[38] Specifically, they proposed a relaxation pathway in which the iodine atom is ejected, leaving behind a dipole-bound water cluster anion. They further hypothesized that the different behavior observed for the photoexcited $I^-(H_2O)_4$ species than for $I^-(H_2O)_5$ or $I^-(H_2O)_6$ is due to differences in the residual energy available to the leaving atom, resulting in fast dynamics (<100 fs) for $n = 4$ and slower dynamics for the larger clusters.

We present herein new theoretical results on the ground and charge-transfer states of the $I^-(H_2O)_4$ cluster that support the proposed crown-like structure and suggest that geometrical relaxation of the water cluster is more important than I atom ejection. This work also goes beyond the earlier theoretical studies of this system in that both singlet and triplet charge-transfer states are considered and the CASSCF/CASPT2 methods[39−44] are used to characterize the excited states. Thus, unlike the study of Chen and Sheu, proper spin-adapted reference functions are employed for the excited states. We recognize from the outset that, given the extended spatial extent of the orbital occupied by the excess electron, the singlet−triplet splittings in the charge-transfer states will be smaller than the spin−orbit interaction of the I atom. Our results on the singlet and triplet states of $I^-(H_2O)_4$ should prove useful as a starting point for future investigations, explicitly accounting for the spin−orbit interactions. Moreover, knowledge of the splittings may be relevant for developing models for the $Cl^-(H_2O)_4$ cluster, for which the spin−orbit interactions are much smaller.

Computational Details

$(H_2O)_4$, in its global potential energy minimum, has a cyclic structure, with each water monomer acting as a single donor and single acceptor.[45] The H atoms of the free OH groups display an up−down−up−down alternating pattern with respect to the plane of the four O atoms so that the molecule has no net dipole moment.[46,47] The $I^-(H_2O)_4$ complex, in its most stable form, is believed to retain the cyclic $(H_2O)_4$ structure but with all four free OH groups pointed toward the I^- ion (see Figure 1). As a result, the $(H_2O)_4$ portion of the complex has a dipole moment (3.65 D in the present calculations) considerably in excess of that needed to bind an excess electron,[48−54] and the charge-transfer excited states of $I^-(H_2O)_4$ are expected to be dipole bound.

Theoretical treatment of dipole-bound anions requires the use of extended basis sets with very diffuse functions as well as the inclusion of electron correlation effects.[55,56] Theoretical characterization of the charge-transfer excited states is further complicated by the inappropriateness of single-determinantal wave functions for providing a correct zeroth-order description

* To whom correspondence should be addressed.
† Present address: Department of Chemistry, University of Washington, Seattle, WA 98195.

10.1021/jp013169n CCC: $22.00
Published on Web 01/25/2002

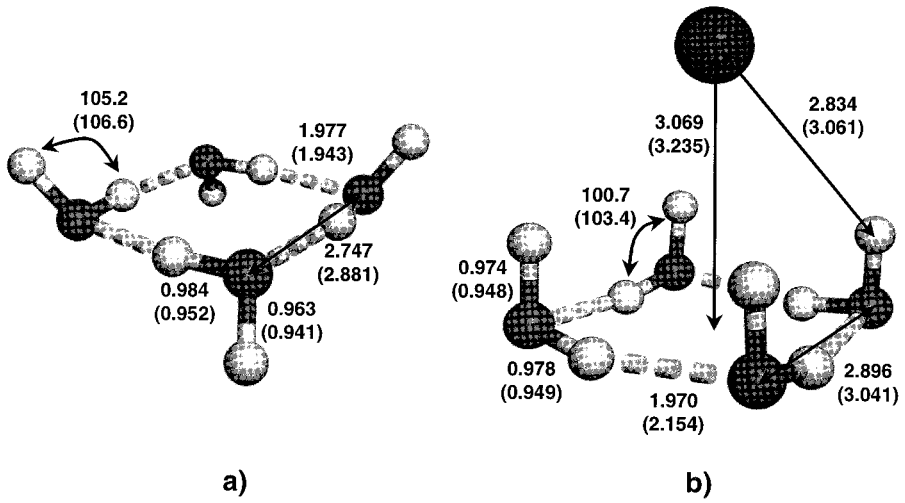

Figure 1. Hartree-Fock (in parentheses) and MP2 optimized structure parameters for (a) $(H_2O)_4$ and (b) $I^-(H_2O)_4$.

of the singlet states. In the present study, this problem is dealt with by use of the CASSCF/CASPT2 procedures.[39−44]

The calculations proceeded as follows. The geometry of the ground state of $I^-(H_2O)_4$ was optimized at the single-reference MP2 level under the constraint of C_4 symmetry, and using a 6-31+G[2d,p][57] description of the water molecules and a modified MIDI! basis set on the I ion.[58] The later was generated from the standard MIDI! basis set by adding diffuse *s* and *p* primitive Gaussian functions with exponents of 0.0439022 and 0.0338511, respectively, and replacing each of the two outermost primitive *d* functions with two two-component contracted functions.[59] The tighter set of *d* functions had exponents of 0.574409 and 0.246533 and contraction coefficients of 0.248065 and 1.072953, respectively. The more diffuse set of *d* functions had exponents of 0.091353 and 0.033851 and contraction coefficients of 0.136634 and 0.054360, respectively. MP2 calculations with the modified MIDI! basis set gave for I an electron affinity of 3.17 eV in good agreement with experimental value of 3.06 eV.[60] These calculations were performed using the Gaussian 98 program.[61]

The optimized geometry of $I^-(H_2O)_4$ was employed in the calculations of the electronically excited states. However, although the mixed basis set described above is sufficiently flexible to describe the ground state of $I^-(H_2O)_4$, the inclusion of still more diffuse functions is required to describe the charge-transfer states. For this purpose, six diffuse Gaussian *sp* functions (with exponents ranging from 0.0076325 to 0.0000216) were added to the I atom basis set. These functions were extracted from a still larger basis set of Gutowski et al. designed to describe a series of dipole-bound anions.[55,56] Although the charge-transfer process gives rise to dipole-bound states associated with the $(H_2O)_4$ portion of the cluster, the orbital occupied by the excess electron is highly delocalized, permitting the diffuse functions to be centered on the I atom.

The charge-transfer states of the $I^-(H_2O)_4$ cluster arise from excitation of an electron from the 5p orbital of the I^- ion to the lowest unoccupied orbital (LUMO) of the water cluster. For the C_4 symmetry equilibrium structure of the anion, the three components of the I 5p orbital are of *a* and *e* symmetry, and the LUMO of the water cluster is of *a* symmetry. Thus there are ^3A, ^3E, ^1A, and ^1E charge-transfer states.

The calculations on the excited states of $I^-(H_2O)_4$ were performed using the CASSCF[39−41] and CASPT2 methods[42−44] as implemented in the MOLCAS program.[62] Our initial CASSCF calculations correlated six electrons, allowing for all rearrangements in the space comprised of the iodine 5p orbitals together with the dipole-bound orbital localized on the water cluster. However, convergence difficulties were encountered when using this procedure, and we adopted, instead, the smallest physically meaningful active space for each state, namely, a single iodine 5p orbital and the dipole-bound orbital. This resulted in a three-configurational wave function for the ground and excited ^1A states and one configurational wave functions for the other states (where the single-configurational wave functions consisted of two Slater determinants to generate proper spin functions). These CASSCF references spaces and orbitals were used in carrying out the CASPT2 calculations.

Potential energy curves for relaxation of the ground and charge-transfer states of $I^-(H_2O)_4$ were calculated using a "reaction" coordinate generated by scanning the dihedral angle between the "crown" H atoms and the plane of the oxygen atoms. For each choice of the scanned dihedral angle (χ), the remaining degrees of freedom were optimized for the ground state, while retaining C_4 symmetry. The resulting geometries were used for single-point calculations on the charge-transfer states. To check the suitability of this reaction coordinate, for the ^3A charge-transfer state we performed exploratory calculations in which both the dihedral angle χ and the distance between the I atom and the plane of the oxygen atoms were varied to generate a potential energy surface (PES). The results of these calculations reveal that the minimum energy path in this PES is dominated by the opening of the dihedral angle, whereas the optimal position of the I atom remains nearly constant.

Results and Discussion

Optimized Structure and Vibrational Frequencies of the Ground State. Figure 1 reports the MP2 optimized structures for the ground states of $(H_2O)_4$ and $I^-(H_2O)_4$. As found in earlier theoretical studies, the interaction of the $(H_2O)_4$ cluster with the I^- ion causes the free OH groups to reorient so that all four free OH groups point toward the I^-. The dihedral angle between the "crown" hydrogen atoms and the plane of the oxygen atoms is predicted to be 80.8°, in good agreement with earlier theoretical predictions. The interaction with the I^- ion causes the free OH groups to lengthen by about 0.01 Å.

The calculated (MP2 level) OH stretch infrared spectrum for the ground state of $I^-(H_2O)_4$ is shown in Figure 2. To correct for the errors introduced by the harmonic approximation, the theoretical spectrum was obtained by shifting the calculated

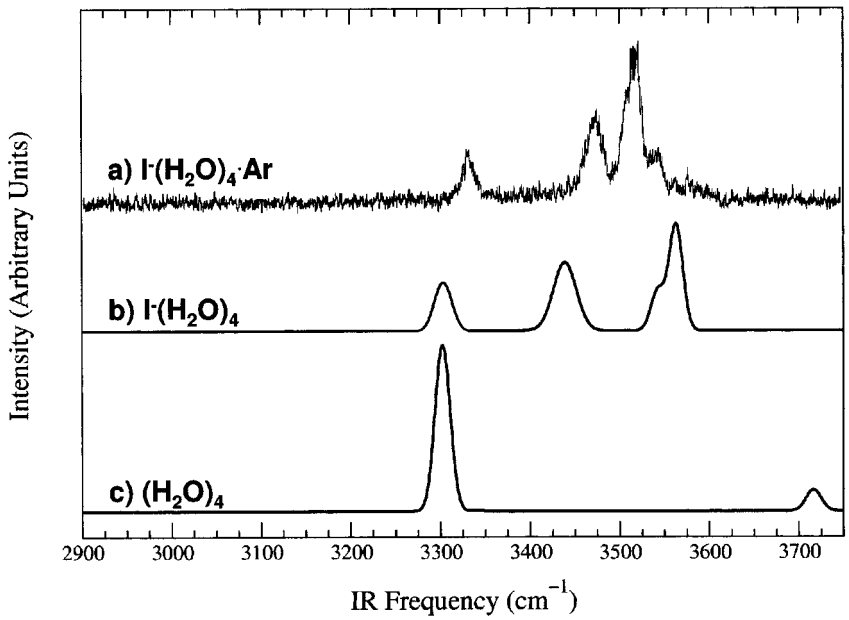

Figure 2. (a) Experimental vibrational spectrum of $I^-(H_2O)_4$.Ar (from ref 63), (b) theoretical vibrational spectrum for $I^-(H_2O)_4$, and (c) theoretical vibrational spectrum for $(H_2O)_4$.

frequencies (of the OH stretch modes) by -190.6 cm^{-1}. This correction corresponds to the difference between the experimental and calculated averages of the symmetric and antisymmetric modes of the water monomer. To facilitate comparison with experiment, a Gaussian envelope corresponding to the theoretical intensity and the experimental bandwidth was added to each OH stretch line. In the simulated spectrum, we have also included a band that is due to the overtones of the HOH bending modes. Again, the frequencies were corrected by the difference between the experimental and calculated frequencies of the bending modes of the water monomer. The intensity of the cluster of bend overtone transitions was taken to be 0.7 times that of the intense single-donor OH stretch vibration. This is the same ratio of the bend to OH stretch fundamental as in the experimental spectrum. For comparison, the figure also includes the experimental spectrum of $I^-(H_2O)_4Ar$[63] as well as the calculated spectrum of $(H_2O)_4$.

The calculated spectrum of $I^-(H_2O)_4$ consists of a pair of closely spaced intense transitions near 3553 cm^{-1} that are due to OH_I stretch vibrations and an intense doubly degenerate transition at 3439 cm^{-1} that is due to OH_S vibrations. (OH_I and OH_S designate the free OH groups pointed to the I^- and the single-donor OH groups, respectively.) In contrast, for $(H_2O)_4$ the intense degenerate transition which is due to the OH_S vibrations is calculated to fall at 3302 cm^{-1}, and the free OH stretch vibrations near 3717 cm^{-1}, with the latter being quite weak. Thus, the interaction with the I^- ion is predicted to cause a shift of about 137 cm^{-1} in the frequency of the intense OH_S vibrations and a larger (≈ -164 cm^{-1}) shift and intensity enhancement in a pair of free OH stretch vibrations.

The experimental IR spectrum of $I^-(H_2O)_4$ displays intense transitions at 3518, 3544, and 3475 cm^{-1}, together with a weaker band at 3331 cm^{-1}. Johnson et al.[20] concluded, on the basis of the comparison of the $I^-(H_2O)_4$ and $I^-(H_2O)_3$ vibrational spectra, that the high frequency doublet is due to OH_I vibrations and that the intense lower frequency transition is due to the degenerate OH_S vibration. The low-frequency transition at 3320 cm^{-1} is expected to derive from an overtone of an HOH bend.[19−23] The surprisingly high intensity of the overtone band is expected to be due to Fermi resonances between the bend overtones and the most red-shifted intense OH stretch modes.

TABLE 1: Excitation and Vertical Detachment Energies (eV) for the Low-Lying Excited States of $I^-(H_2O)_4$

		excitation energy		VDE	
system	state	CASSCF	CASPT2	CASSCF	CASPT2
$I(H_2O)_4$	1^2A	4.087	4.628		
$I(H_2O)_4$	1^2E	4.072	4.630		
$I^-(H_2O)_4$	1^3A	4.065	4.582	0.022	0.046
$I^-(H_2O)_4$	1^3E	4.051	4.582	0.037	0.046
$I^-(H_2O)_4$	2^1A	4.073	4.599	0.015	0.029
$I^-(H_2O)_4$	1^1E	4.056	4.598	0.031	0.030

This mechanism has been found to account for the high intensity of the HOH bending overtones of $X^-(H_2O)$ complexes.[64]

The splitting between the intense OH_S and OH_I transitions in the calculated spectrum is considerably greater than that in the experimental spectrum (114 vs. 69 cm^{-1}). This is a result of the tendency of the MP2 method to exaggerate the weakening of the OH_S bonds for extended H-bond networks as in the $(H_2O)_4$ ring.[65,66] Although this problem is remedied by inclusion of high-order electron correlation effects, e.g., by use of the QCISD(T) method,[66] such calculations would be prohibitively expensive for $I^-(H_2O)_4$. An alternative approach, which has proven successful for the neutral clusters is to scale the MP2-level frequency shifts associated with the OH_S vibrations by a factor of 0.73.[66] Application of this correction to $I^-(H_2O)_4$ reduces the splitting between the OH_W and OH_I modes to 52 cm^{-1}, in good agreement with experiment. In concluding this section, we note that an MP2-level vibrational spectrum of $I^-(H_2O)_4$ was recently reported by Lee and Kim.[67] Although the calculated spectrum of these authors corresponds closely to that reported here, they concluded that there was not good agreement between the calculated and measured spectra. Apparently, this is due to their attributing the observed band at 3331 cm^{-1} to an OH stretch mode rather than to overtones of bending modes.

Excitation and Vertical Detachment Energies. Table 1 reports the calculated vertical electronic excitation energies of $I^-(H_2O)_4$ together with the detachment energies associated with the charge-transfer excited states. The latter were obtained by subtracting the energies of the excited states of $I^-(H_2O)_4$ from that of $I(H_2O)_4$ in its 1^2A ground state. All energies were

calculated using the MP2/MIDI! optimized geometry of the ground-state anion.

The triplet states are calculated to lie energetically below the singlet states by about 8 and 15 meV at the CASSCF and CASPT2 levels, respectively, and the A and E states are predicted to be nearly degenerate in both the triplet and singlet manifolds. The CASSCF method gives a value of 4.07 eV for the $1^1A \rightarrow 2^1A$ excitation energy. This increases to 4.60 eV with the CASPT2 method. The latter result is in good agreement with other theoretical calculations including dynamical electron correlation effects (i.e., 4.44 and 4.40 eV from TD-DFT[36] and single-reference MP2[37] calculations, respectively) and also with the experimental value of 4.45 ± 0.05 eV.[33] The CASPT2 calculations also give an ionization energy $I^-(H_2O)_4$ in good agreement with experiment, with the calculated IP for the $1^1A \rightarrow 1^2A$ transition being 4.68 eV compared to the measured IP of 4.59 ± 0.02 eV.[16]

For the 2^1A charge-transfer state, the CASSCF and CASPT2 calculations give detachment energies of 15 and 29 meV, respectively. Somewhat larger values were reported by Chen and Sheu, but in part, this is due to their use of single-determinant-based Hartree−Fock and MP2 methods for describing the charge-transfer state, which has the effect of mixing the singlet and triplet states. On the basis of the results of photodetachment experiments, Serxner et al.[33] deduced a value of 100 meV for the vertical detachment energy for the charge transfer states, whereas Lehr et al.[34] arrived at an estimate of 190 ± 140 meV for the VDE from their initial time electron kinetic energy decay measurements. An error estimate was not reported by Serxner et al., but on the basis of the procedure used to deduce the detachment energy, we conclude that it is at least 50 meV. Thus, although there is sizable uncertainty in the experimental value of the vertical detachment energies of the charge transfer states, it does appear as though our calculations underestimate this quantity. There are several factors that could contribute to an underestimation of the stability of the charge-transfer states. These include (1) the neglect of spin−orbit effects, (2) the neglect of higher-order correlation effects, and (3) errors in the geometry used in the calculations. Spin−orbit effects are expected to be of comparable importance for the charge-transfer states and for the $I(H_2O)_4$ neutral molecule and, thus, are likely to be relatively unimportant for the detachment energies. Of the other two factors, the neglect of higher-order electron correlation effects are expected to be particularly important, because they have been found to be important for electron binding to the neutral clusters.[68,69]

Finally, it should be noted that, even though the calculations give a spread in detachment energies owing to the existence of four charge-transfer states and two closely spaced states of the neutral cluster, the splittings would not be resolved under the experimental conditions. Indeed, they would be considerably modified by spin−orbit interactions.

Potential Energy Curves. Figure 3 presents the CASSCF and CASPT2 potential energy curves for the ground state of $I^-(H_2O)_4$ along the previously described deformation coordinate χ. For both theoretical approaches, the potential energy minimum is predicted to occur for χ close to 80°. Figures 4 and 5 report the calculated potential energy curves of the excited states of $I^-(H_2O)_4$ as well as for the lowest energy ^2E and ^2A states of $I(H_2O)_4$. For comparison, the corresponding HF and MP2-level potential energy curves of $(H_2O)_4$ and $(H_2O)_4^-$ have been included. The latter curves were generated using the same reaction coordinate and basis set as employed for $I^-(H_2O)_4$ (i.e., including the diffuse functions that were centered on the I atom in the $I^-(H_2O)_4$ cluster).

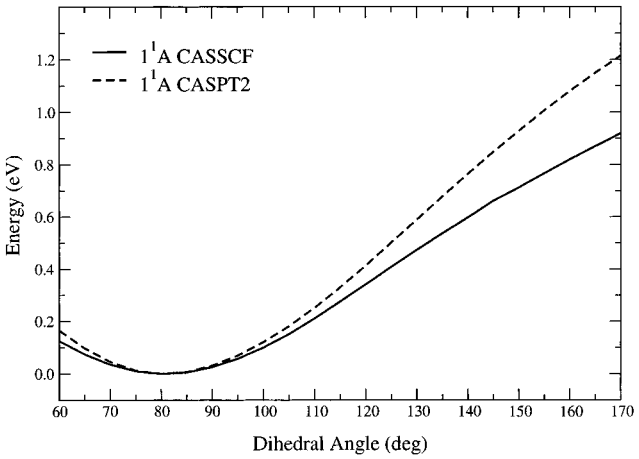

Figure 3. CASSCF and CASPT2 potential energy curves for the ground state of $I^-(H_2O)_4$.

Both the CASSCF and CASMP2 calculations predict the charge-transfer anion states to be bound (i.e., lie energetically below the neutral curves) from the smallest dihedral angle considered (60°) out to a dihedral angle of about 160°. The energy separation between the anionic charge-transfer states and the ground state of the neutral cluster decreases with increasing dihedral angle. This is due to the falloff in the dipole moment of the neutral cluster with increased "flattening" of the water portion of the cluster.

In the vertical excitation region (i.e., at the geometry of the ground state of the anion), the potential energy curves of the charge-transfer states are repulsive. In both the singlet and triplet manifolds and for both the CASSCF and CASPT2 methods, the A and E states are predicted to cross near a χ value of 83°. This is close to the χ value at which the ground state anion has its potential energy minimum, thereby explaining the near degeneracy of the A and E states reported in Table 1. The stabilization of the A states relative to the E states for small dihedral angles is presumably a result of delocalization of the electron associated with the dipole-bound orbital of the water cluster into the partially occupied p_z orbital of the I atom. The CASSCF and CASPT2 potential energy curves of the charge-transfer states differ in that the CASPT2 potentials have shallow local minima near $\chi = 125°$ which are absent in the CASSCF potential energy curves. The minima are calculated to lie energetically about 4.1 eV above the ground-state anion, close to the 4.05 eV experimental onset of the photodetachment spectrum.[33]

As noted above, vertical excitation from the ground state of $I^-(H_2O)_4$ produces the charge transfer states in a region of the potential which is repulsive along the χ coordinate. As a result, the system is expected to rapidly evolve along this coordinate and, after a short time, to encounter geometries at which the neutral and anion states are degenerate and electron detachment can occur. This channel would also be highly favored by the small mass of the hydrogen atoms. Therefore, we expect electron autoionization to be more important decay channel than the $I + (H_2O)_4^-$ channel proposed by Chen and Sheu.[38]

We now examine the potential energy curves (along the χ coordinate) of the cyclic $(H_2O)_4$ cluster and its dipole-bound anion. Although the Hartree−Fock potential energy curves for these species are dissociative, the corresponding MP2 level potential energy curves possess shallow minimum near 133 and 122°, respectively. This is reminiscent of the situation for

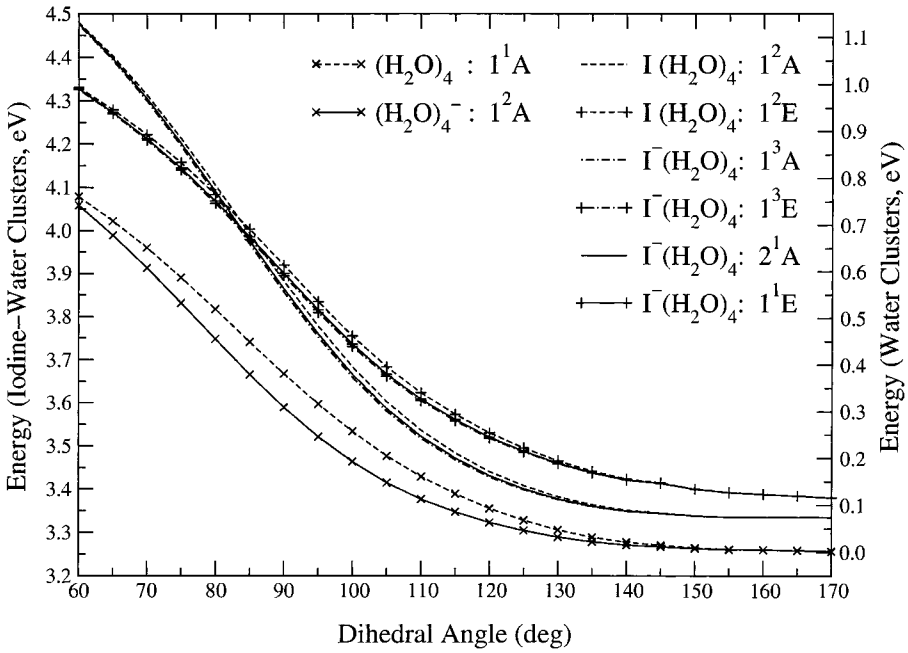

Figure 4. CASSCF potential energy curves for the low-lying states of $I^-(H_2O)_4$, $I(H_2O)_4$, $(H_2O)_4^-$, and $(H_2O)_4$.

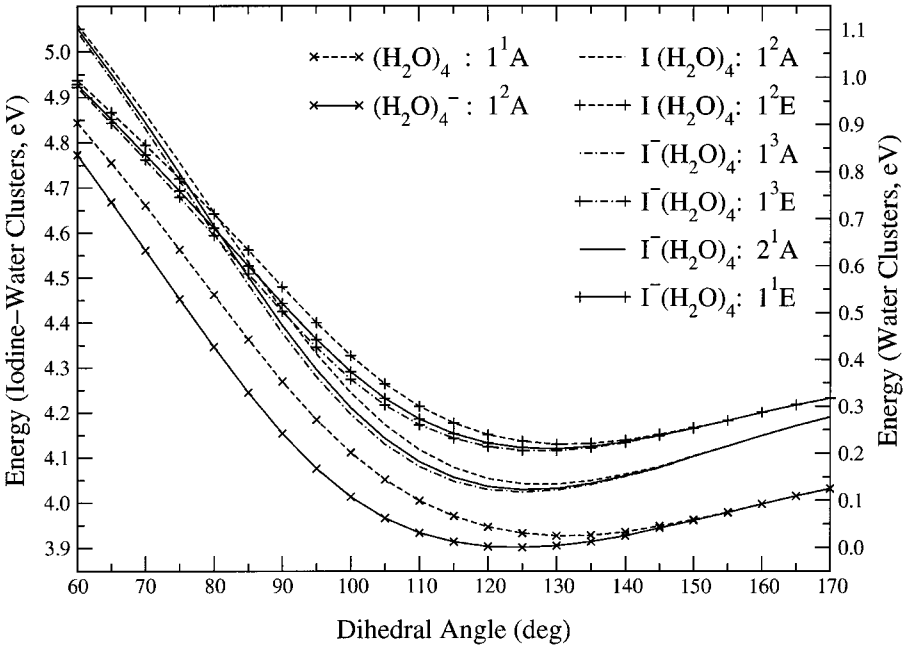

Figure 5. CASPT2 potential energy curves for the low-lying states of $I^-(H_2O)_4$, $I(H_2O)_4$, $(H_2O)_4^-$, and $(H_2O)_4$.

$I(H_2O)_4$ and $I^-(H_2O)_4$, discussed above. Because the geometry optimizations were constrained, these results do not establish whether the crown structures of $(H_2O)_4$ and $(H_2O)_4^-$ are true potential energy minima. In fact, in the case of the neutral cluster, it is clear from the outset that the crown structure cannot be a true local minimum. This is confirmed by carrying out an unconstrained geometry optimizations starting with the crown structure from the constrained optimization. On the other hand, analogous calculations on $(H_2O)_4^-$ show that it does possess a local minimum with a crown-like structure.

Detachment Energy and Dipole Moment Curves. Figure 6 reports the variation of the electron detachment energies of the charge-transfer states of $I^-(H_2O)_4$ and of the ground state of $(H_2O)_4^-$ as a function of the torsional angle χ. The corresponding dipole moment curves are reported in Figure 7. The dipole moment necessarily goes to zero as $\chi \rightarrow 0$ or 180°. For both $(H_2O)_4$ and $I(H_2O)_4$, the dipole moment peaks near $\chi = 110°$. (As discussed below, the detachment energy peaks at a somewhat smaller χ value.) For a given value of χ, the detachment energy of $(H_2O)_4^-$ is significantly larger than the detachment energies associated with the charge-transfer states of $I^-(H_2O)_4$. The weaker electron binding in the latter species is a consequence of the exclusion of the weakly bound electron from the region of space occupied by the I atom, as noted previously by Chen and Sheu.[38] Our analysis of the electron density shows that the optimal position of the I atom in $I^-(H_2O)_4$ corresponds roughly to the maximum of the excess electron density in $(H_2O)_4^-$. Therefore, when an I atom is introduced into this system, the excess electron is pushed away from the $(H_2O)_4$ moiety and the binding energy is significantly reduced.

Although the dipole moment curve of $(H_2O)_4$ has its a maximum near $\chi = 110°$, the detachment energy has its

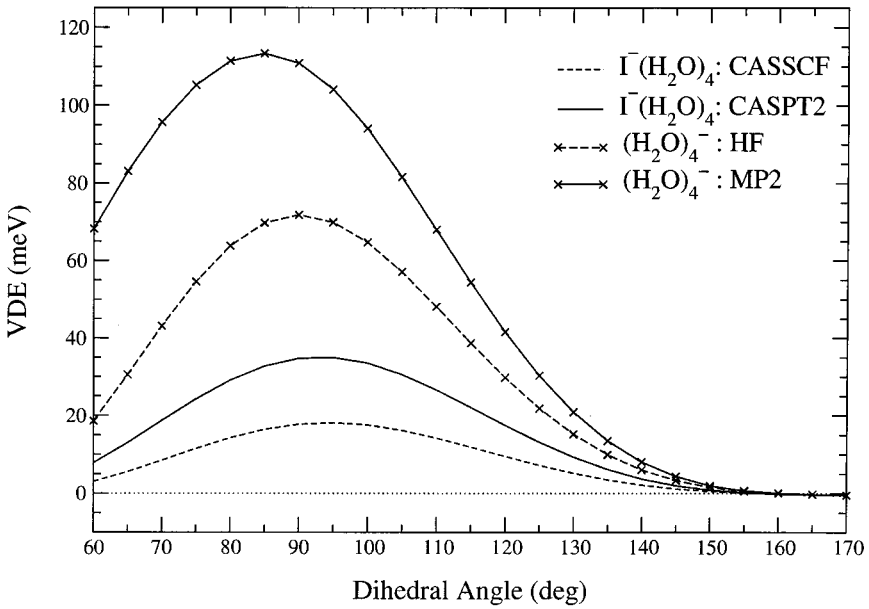

Figure 6. Vertical detachment energy curves for $I^-(H_2O)_4$ and $(H_2O)_4^-$.

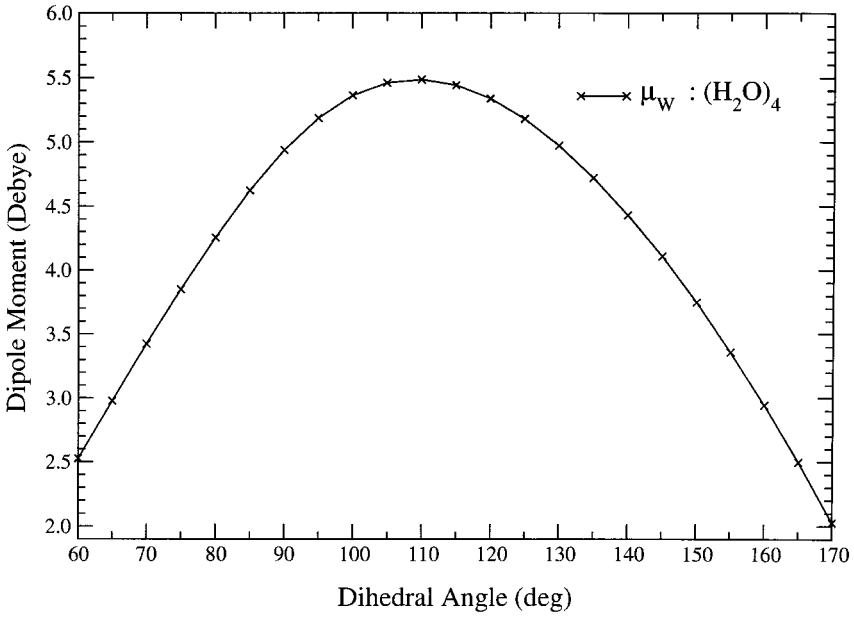

Figure 7. Dipole moment calculated at the MP2 level for $(H_2O)_4$ as a function of the dihedral angle χ.

maximum near $\chi = 90°$. Moreover, for $\chi = 60°$, for which the dipole moment is only about 2.5 D, the electron binding energy remains sizable ($\approx$70 meV). This is much larger than would be expected were only the dipole field involved in the electron binding. It appears that at these smaller angles higher moments in the net electrostatic potential are playing a significant role in the electron binding. In addition, the nearly 3.5-fold increase in the electron binding energy in going from the Hartree−Fock to the MP2 level of theory (at $\chi = 60°$) indicates that electron−molecule dispersion interactions are also playing an important role in the electron binding.[68]

Conclusions

Ab initio electronic structure calculations have been used to characterize the ground and low-lying excited states of $I^-(H_2O)_4$. Our calculated infrared spectrum for the ground-state anion is in good agreement with the measured spectrum, providing support for the crown-like structure for $I^-(H_2O)_4$. The CASPT2 procedure is used to characterize the charge-transfer states of $I^-(H_2O)_4$ as a function of the dihedral angle that determines the extent to which the H atoms of the free OH groups are displaced from the plane of the O atoms. The calculations predict the splittings between the singlet and triplet charge-transfer states to be only about 15 meV at the geometry of the neutral molecule. This is much less than the expected spin−orbit splittings. The calculated excitation and electron detachment energies are in good agreement with experiment.

The calculations also show that the potential energy curves for the charge-transfer states are repulsive in the vertical excitation region. Moreover, even though there are shallow minima in these potential energy curves, sufficient energy is deposited into the system by vertical excitation that both the $I + (H_2O)_4^-$ and $I(H_2O)_4 + e^-$ decay channels are accessible. We expect the latter to dominate since the molecule only needs to open up to a χ value of about 130° for electron autoionization to occur. At this χ value, the I atom has moved only about 0.5

Å further from the plane of the four O atoms (compared to its position in the minimum energy structure of the ground state anion). Finally, we note that an excess electron binds much more strongly to the crown-shaped $(H_2O)_4$ molecule than to $I(H_2O)_4$. This is due to the "excluded volume" effect of the I atom.

Acknowledgment. This research was carried out with the support of the National Science Foundation. The calculations were carried out on the IBM RS6000 cluster in the University of Pittsburgh's Center for Molecular and Materials Simulations and which were funded by IBM and NSF. We acknowledge valuable discussions with Professors M. Johnson and D. Neumark.

References and Notes

(1) Keene, J. P. *Nature* **1960**, *188*, 843.
(2) Keene, J. P. *Nature* **1963**, *197*, 47.
(3) Hart, E. J.; Boag, J. W. *J. Am. Chem. Soc.* **1962**, *84*, 4090.
(4) Boag, J. W.; Hart, E. J. *Nature* **1963**, *197*, 45.
(5) Wiesenfeld, M.; Ippen, E. P. *Chem. Phys. Lett.* **1980**, *73*, 47.
(6) Mingus, A.; Gauduel, Y.; Martin, J. L.; Antonetti, A. *Phys. Rev. Lett.* **1987**, *80*, 1559.
(7) Gauduel, Y.; Pommeret, S.; Yamada, N.; Migus, A.; Antonetti, A. *Ultrafast Phenomena VII*; Harris, C. B., Ippen, E. P., Mourou, G. A., Zewail, A. H., Eds., Springer-Verlag: New York, 1990.
(8) Silva, C.; Walhout, P. K.; Yokoyama, K.; Barbara, P. F. *Phys. Rev. Lett.* **1998**, *80*, 1086.
(9) Schwartz, B. J.; Rossky, P. J. *J. Phys. Chem.* **1994**, *98*, 4489.
(10) Space, B.; Coker, D. F. *J. Chem. Phys.* **1992**, *96*, 652.
(11) Sheu, W.-S.; Rossky, P. J. *Chem. Phys. Lett.* **1993**, *213*, 233.
(12) Staib, A.; Borgis, D. *J. Chem. Phys.* **1996**, *104*, 9027.
(13) Frank, J.; Scheibe, G. *Z. Phys. Chem. A* **1928**, *139*, 22.
(14) Jortner, J.; Ottolenghi, M.; Stein, G. *J. Phys. Chem.* **1964**, *68*, 247.
(15) Schwartz, B. J.; Bittner, E. R.; Prezhdo, O. V.; Rossky, P. J. *J. Chem. Phys.* **1996**, *104*, 5942.
(16) Markovich, G.; Giniger, R.; Levin, M.; Cheshnovsky, O. *J. Chem. Phys.* **1991**, *95*, 9416.
(17) Markovich, G.; Pollack, S.; Giniger, R.; Cheshnovsky, O. *J. Chem. Phys.* **1994**, *101*, 9344.
(18) Achatz, U.; Joos, S.; Berg, C.; Beyer, M.; Niedner-Schatteburg, G.; Bondybey, V. E. *Chem. Phys. Lett.* **1998**, *291*, 459.
(19) Ayotte, P.; Weddle, G. H.; Kim, J.; Johnson, M. A. *J. Am. Chem. Soc.* **1998**, *120*, 12361.
(20) Ayotte, P.; Bailey, C. G.; Weddle, G. H.; Johnson, M. A. *J. Phys. Chem. A* **1998**, *102*, 3067.
(21) Ayotte, P.; Weddle, G. H.; Kim, J.; Kelley, J.; Johnson, M. A. *J. Phys. Chem. A* **1999**, *103*, 443.
(22) Ayotte, P.; Nielsen, S. B.; Weddle, G. H.; Johnson, M. A. *J. Phys. Chem. A* **1999**, *103*, 10665.
(23) Ayotte, P.; Weddle, G. H.; Johnson, M. A. *J. Chem. Phys*. **1999**, *110*, 7129.
(24) Coe, J. V.; Lee, G. H.; Eaton, J. G.; Arnold, S. T.; Sarkas, H. W.; Bowen, K. H.; Ludewigt, C.; Haberland, H.; Worsnop, D. R. *J. Chem. Phys.* **1990**, *92*, 3980.
(25) Lee, G. H.; Arnold, S. T.; Eaton, J. G.; Sarkas, H. W.; Bowen, K. H.; Ludewigt, C.; Haberland, H. *Z. Phys. D* **1991**, *20*, 9.
(26) Kim, J.; Becker, I.; Cheshnovsky, O.; Johnson, M. A. *Chem. Phys. Lett.* **1998**, *297*, 90.
(27) Ayotte, P.; Johnson, M. A. *J. Chem. Phys.* **1997**, *106*, 811.
(28) Campagnola, P. J.; Lavrich, D. J.; Deluca, M. J.; Johnson, M. A. *J. Chem. Phys.* **1991**, *94*, 5240.
(29) Maeyama, T.; Tsumura, T.; Fujii, A.; Mikami, N. *Chem. Phys. Lett.* **1997**, *264*, 292.
(30) Barnett, R. N.; Landman, U.; Cleveland, C. L.; Jortner, J. *J. Chem. Phys.* **1988**, *88*, 4421.
(31) Kim, K. S.; Lee, S.; Kim, J.; Lee, J. Y. *J. Am. Chem. Soc.* **1997**, *119*, 9329.
(32) Ayotte, P.; Weddle, G. H.; Bailey, C. G.; Johnson, M. A.; Vila, F.; Jordan, K. D. *J. Chem. Phys.* **1999**, *110*, 6268.
(33) Serxner, D.; Dessent, C. E.; Johnson, M. A. *J. Chem. Phys.* **1996**, *105*, 7231.
(34) Lehr, L.; Zanni, M. T.; Frischkorn, C.; Weinkauf, R.; Neumark, D. M. *Science* **1999**, *284*, 635.
(35) Frischkorn, C.; Zanni, M. T.; Davis, A. V.; Neumark, D. M. *Faraday Discuss.* **2000**, *115*, 49.
(36) Majumdar, D.; Kim, J.; Kim, K. S. *J. Chem. Phys.* **2000**, *112*, 101.
(37) Chen, H.-Y.; Sheu, W.-S. *J. Am. Chem. Soc.* **2000**, *122*, 7534.
(38) Chen, H.-Y.; Sheu, W.-S. *Chem. Phys. Lett.* **2001**, *335*, 475.
(39) Roos, B. O. *Int. J. Quantum Chem.* **1980**, *S14*, 175.
(40) Roos, B. O.; Taylor, P. R.; Siegbahn, P. E. M. *Chem. Phys.* **1980**, *48*, 157.
(41) Roos, B. O. *Advances in Chemical Physics: Ab Initio Methods in Quantum Chemistry-II*; Lawley, K. P., Ed.; John Wiley & Sons Ltd.: Chichester, U.K., 1987.
(42) Andersson, K.; Malmqvist, P.-Å.; Roos, B. O.; Sadlej, A. J.; Wolinski, K. *J. Phys. Chem.* **1990**, *94*, 5483.
(43) Andersson, K.; Malmqvist, P.-Å.; Roos, B. O. *J. Chem. Phys.* **1992**, *96*, 1218.
(44) Andersson, K.; Roos, B. O. *Modern Electron Structure Theory*; Yarkony, R., Ed.; World Scientific Publishing: New York, 1994; Vol. 1.
(45) Combariza, J. E.; Kestner, N. R.; Jortner, J. *J. Chem. Phys.* **1994**, *100*, 2851.
(46) Kim, K.; Jordan, K. D.; Zwier, T. S. *J. Am. Chem. Soc.* **1994**, *116*, 11568.
(47) Liu, K.; Gregory, J. K.; Brown, M. G.; Carter, C.; Saykally, R. J.; Clary, D. C. *Nature* **1996**, *381*, 501.
(48) Fermi, F.; Teller, E. *Phys. Rev.* **1947**, *72*, 399.
(49) Crawford, O. H. *Proc. R. Soc. London* **1967**, *91*, 279.
(50) Crawford, O. H.; Dalgarno, A. *Chem. Phys. Lett.* **1967**, *1*, 23.
(51) Brown, W. B.; Roberts, R. E. *J. Chem. Phys.* **1967**, *46*, 2006.
(52) Garrett, W. R. *Phys. Rev.* A **1971**, *3*, 961.
(53) Garrett, W. R. *J. Chem. Phys.* **1980**, *73*, 5721.
(54) Garrett, W. R. *J. Chem. Phys.* **1982**, *77*, 3666.
(55) Gutowski, M.; Skurski, P.; Jordan, K. D.; Simons, J. *Int. J. Quantum Chem.* **1997**, *64*, 183.
(56) Gutowski, M.; Skurski, P.; Boldyrev, A. I.; Simons, J.; Jordan, K. D. *Phys. Rev.* A **1996**, *54*, 1906.
(57) The 6-31+G[2d,p] basis set is a hybrid in which the core-valence and diffuse exponents are taken from the 6-31+G(d,p) basis set (Hariharan, P. C.; Pople, J. A. *Theor. Chim. Acta* **1973**, *28*, 213. Gill, P. M. W.; Johnson, B. G.; Pople, J. A.; Frisch, M. J. *Chem. Phys. Lett.* **1992**, *197*, 499), whereas the polarization exponents are taken from the aug-cc-pVDZ basis set (Dunning, T. H., Jr. *J. Chem. Phys.* **1989**, *90*, 1007). See also ref 32.
(58) Li, B. J.; Cramer, C. J.; Truhlar, D. G. *Theor. Chem. Acc.* **1998**, *99*, 192.
(59) Sadlej, A. J. *Theor. Chim. Acta* **1992**, *81*, 339.
(60) Hanstorp, D.; Gustafsson, M. *J. Phys. B* **1992**, *25*, 1773.
(61) Frisch, M. J.; Trucks, G. W.; Schlegel, H. B.; Scuseria, G. E.; Robb, M. A.; Cheeseman, J. R.; Zakrzewski, V. G.; Montgomery, J. A., Jr.; Stratmann, R. E.; Burant, J. C.; Dapprich, S.; Millam, J. M.; Daniels, A. D.; Kudin, K. N.; Strain, M. C.; Farkas, O.; Tomasi, J.; Barone, V.; Cossi, M.; Cammi, R.; Mennucci, B.; Pomelli, C.; Adamo, C.; Clifford, S.; Ochterski, J.; Petersson, G. A.; Ayala, P. Y.; Cui, Q.; Morokuma, K.; Malick, D. K.; Rabuck, A. D.; Raghavachari, K.; Foresman, J. B.; Cioslowski, J.; Ortiz, J. V.; Stefanov, B. B.; Liu, G.; Liashenko, A.; Piskorz, P.; Komaromi, I.; Gomperts, R.; Martin, R. L.; Fox, D. J.; Keith, T.; Al-Laham, M. A.; Peng, C. Y.; Nanayakkara, A.; Gonzalez, C.; Challacombe, M.; Gill, P. M. W.; Johnson, B. G.; Chen, W.; Wong, M. W.; Andres, J. L.; Head-Gordon, M.; Replogle, E. S.; Pople, J. A. *Gaussian 98*, revision A.7; Gaussian, Inc.: Pittsburgh, PA, 1998.
(62) Andersson, K.; Blomberg, M. R. A.; Fülscher, M. P.; Karlström, G.; Lindh, R.; Malmqvist, P.-Å.; Neogrády, P.; Olsen, J.; Roos, B. O.; Sadlej, A. J.; Schütz, M.; Seijo, L.; Serrano-Andrés, L.; Siegbahn, P. E. M.; Widmark, P.-O. *MOLCAS*, version 4; Lund University: Lund, Sweden, 1997.
(63) Weber, J. W.; Kelley, J. A.; Robertson, W. H.; Johnson, M. A. *J. Chem. Phys.* **2001**, *14*, 2698.
(64) Robertson, W. H.; Weddle, G. H.; Kelley, J. A.; Johnson, M. A. Unpublished results.
(65) Frochtenicht, R.; Kaloudis, M.; Koch, M.; Huisken, F. *J. Chem. Phys.* **1996**, *105*, 6128.
(66) Jordan, K. D. Unpublished results.
(67) Lee, H. M.; Kim, K. S. *J. Chem. Phys.* **2001**, *114*, 4461.
(68) Gutowski, M.; Jordan, K. D.; Skurski, P. *J. Phys. Chem.* **1998**, *102*, 2624.
(69) Wang, F.; Jordan, K. D. Unpublished results.